

# Continued Fractions and the 4-Color Theorem

Richard Evan Schwartz \*

August 9, 2022

## Abstract

We study the geometry of some proper 4-colorings of the vertices of sphere triangulations with degree sequence  $6, \dots, 6, 2, 2, 2$ . Such triangulations are the simplest examples which have non-negative combinatorial curvature. The examples we construct, which are roughly extremal in some sense, are based on a novel geometric interpretation of continued fractions. We will also present a conjectural sharp “isoperimetric inequality” for colorings of this kind of triangulation.

## 1 Introduction

### 1.1 Background

The Four Color Theorem, first proved (with the assistance of a computer) by Wolfgang Haken and Kenneth Appel in 1976, is one of the most famous results in mathematics. See [W] for a thorough discussion. Here is one formulation. If you have any triangulation of the 2-sphere, it is possible to color the vertices using 4 colors such that no two adjacent vertices have the same coloring. This is called a *proper vertex 4-coloring*.

Certainly one can properly 4-color the vertices of a tetrahedron. A proper vertex 4-coloring of a triangulation  $\mathcal{Z}$  (with the same colors) canonically defines a simplicial map  $f$  from the sphere to the tetrahedron: Just map each vertex of  $\mathcal{Z}$  to the like-colored vertex of the tetrahedron and then extend linearly to the faces. The map  $f$  in turn defines a 2-coloring of the faces of

---

\*Supported by N.S.F. Grant DMS-2102802

$\mathcal{Z}$ . One colors a face of  $\mathcal{Z}$  black if  $f$  is orientation preserving on that face, and otherwise white.

The associated face 2-coloring has the property that around each vertex the number of black faces is congruent mod 3 to the number of white faces. This derives from the property that 3 triangles of the tetrahedron meet around each vertex. We call a face 2-coloring with this property a *good coloring*. Conversely, a good coloring for  $\mathcal{Z}$  defines a simplicial map to the tetrahedron and thus a proper 4-coloring of the vertices of  $\mathcal{Z}$ . So, an equivalent formulation of the 4-color theorem is that every triangulation of the sphere has a good coloring.

So far, the Four Color Theorem only has computer-assisted proofs. Perhaps one can get insight into the result by looking at examples of good colorings. The good coloring version has a geometric feel to it, and so perhaps some geometric insight might help. The purpose of this paper is to look at the geometry of these good colorings in some special cases.

A *triangulation of non-negative combinatorial curvature* is one in which the maximum degree is 6. All the vertices have degree 6 except for a list  $v_1, \dots, v_k$  which have degrees  $d_1, \dots, d_k < 6$ . Euler's Formula gives the condition on the degrees:

$$\sum_{i=1}^k (6 - d_i) = 12. \tag{1}$$

In particular  $k \leq 12$ . The quantity

$$\frac{\pi}{3} \times (6 - d_i)$$

is the *combinatorial curvature* at  $v_i$ . Equation 1 translates into a discrete version of the Gauss-Bonnet theorem, which says that the total combinatorial curvature is  $4\pi$ .

The triangulations of non-negative combinatorial curvature form an attractive family to study. In [T], William Thurston organized these triangulations into moduli spaces. To give some idea of how this works, a triangulation non-negative combinatorial curvature defines a flat cone structure on the sphere with non-negative curvature: we just make all the triangles unit equilateral triangles. The set of all triangulations with the same list  $d_1, \dots, d_k$  of defects includes in the moduli space of flat cone structures on spheres with appropriately prescribed singularities. So, even though the triangulations don't exactly vary continuously, one can think of them as special points inside moduli spaces consisting of structures which do vary continuously. Also,

if the triangulations are large and the defects are well spread out, one can imagine that the defects almost vary continuously.

Given the nice structure of the totality of such triangulations, it seems like an interesting idea to study the space of good colorings as a kind of partially defined bundle over these moduli spaces. Perhaps the structure of such colorings is related somehow to the placement of the defects. As the defects vary around, perhaps the good colorings vary in a nice way to some extent. I imagine that the total picture, seen all at once, would be spectacularly beautiful. All this is very speculative. In spite of making a lot of computer experiments over the years – every time I teach the graph theory class at Brown I play with this project – I don't have much to report. In this very modest paper I will consider the simplest cases. The cases I have in mind are where  $k = 3$  and  $d_1 = d_2 = d_3 = 2$ .

## 1.2 The Continued Fraction Colorings

The  $6, \dots, 6, 2, 2, 2$  triangulations are indexed by the nonzero Eisenstein integers. An *Eisenstein integer* is a number of the form

$$a + b\alpha, \quad a, b \in \mathbf{Z}, \quad \alpha = \frac{1 + i\sqrt{3}}{2}.$$

To see the connection, let  $\mathcal{E}$  denote the ring of Eisenstein integers. The points of  $\mathcal{E}$  are naturally the vertices of an equilateral triangulation  $\mathcal{T}$  of  $\mathbf{C}$ . Given some nonzero  $\beta \in \mathcal{E}$ , the ideal

$$\mathcal{E}_\beta = \{\beta\gamma \mid \gamma \in \mathcal{E}\}$$

consists of the vertices of the larger equilateral triangulation  $\beta\mathcal{T}$ . We let  $G_\beta$  denote the group of symmetries generated by order 3 rotations in the vertices of  $\beta\mathcal{T}$ . The quotient

$$\mathcal{T}(\beta) = \mathcal{T}/G_\beta$$

is the desired triangulation.

Since all the vertices of  $\mathcal{T}(\beta)$  have even degree,  $\mathcal{T}(\beta)$  always has a good coloring. One just colors the triangles alternately black and white in a checkerboard pattern. Indeed, this face coloring corresponds to a proper 3-coloring of the vertices.

Figure 1 shows a different good coloring for  $\beta = 2 + 3\alpha$ . We call this coloring  $\mathcal{C}(2+3\alpha)$ . To get the triangulation of the sphere, cut out the specially

outlined central rhombus, fold it up like a taco, and glue the edges together in pairs. Figure 1 is really showing part of the orbifold universal cover of the coloring. Figures 7 and 8 below show more elaborate examples.

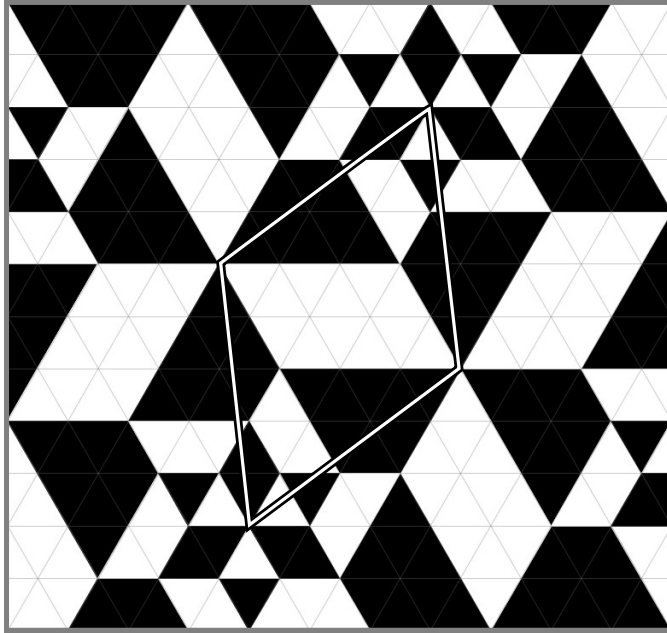


**Figure 1:** The good coloring  $\mathcal{C}(2 + 3\alpha)$  of  $\mathcal{T}(2 + 3\alpha)$ .

The coloring in Figure 1 is (at least experimentally) extremal in a certain sense. Define the *fold count* of a good coloring to be the number of edges which form black-white interfaces. For the alternating coloring, the fold count is  $3/2$  times the number of faces. For  $\mathcal{T}(2 + 3\alpha)$  this comes to 57. In contrast,  $\mathcal{C}(2 + 3\alpha)$  has fold count 23. It seems that  $\mathcal{C}(2 + 3\alpha)$  minimizes the fold count amongst all good colorings of  $\mathcal{T}(2 + 3\alpha)$ .

The number of good colorings of  $\mathcal{T}(\beta)$  grows exponentially with  $|\beta|$ , for an easy reason. In any good coloring, if we can find a vertex of degree 6 where the colors alternate, we can switch the colors and get another good coloring. In terms of the original vertex coloring, the neighbors of such a vertex  $v$  are colored using just 2 colors, and so we have an option to switch the color of  $v$  to the other available color. Starting with the alternating coloring, we can take a large family of non-adjacent vertices and make these swaps according to any binary sequence we like. On the other hand, these examples seem rather similar to the alternating coloring. Their fold count is linear in the number of the faces.

The colorings with smaller fold counts, and in particular with minimal fold counts, seem to be much more rigid and interesting. To use an analogy from statistical mechanics, the colorings with large fold count are sort of like a fluid or a gas, and the colorings with small fold count are more like solid crystals. The example in Figure 1 is part of an infinite sequence of examples. We call these examples  $\mathcal{C}(\beta)$ , where  $\beta$  ranges over the primitive Eisenstein integers. (An Eisenstein integer  $\beta = a + b\alpha$  *primitive* if it is not an integer multiple of another one. Equivalently,  $a$  and  $b$  are relatively prime.) We will see that  $\mathcal{C}(\beta)$  is a special good coloring of  $\mathcal{T}(\beta)$  which geometrically implements the continued fraction expansion of  $a/b$ . We call these colorings *continued fraction colorings*.

### 1.3 Properties of the Continued Fraction Colorings

The main result of this paper is that these continued fraction colorings exist, but I will prove some additional results about them. Here is our first result.

**Theorem 1.1** *Each continued fraction coloring has the same total number of black and white triangles.*

Put more geometrically, the simplicial maps to the sphere defined by the continued fraction colorings have degree 0. Looking at the pictures like Figure 1, you can see that the black and white triangles are distributed differently, so this is not an obvious consequence of symmetry. The proof boils down to an equality satisfied by the orbit of a rational number in  $(0, 1)$  under the so-called slow Gauss map. (See §2.1 for a definition.) The equality is much in the same style as the fact that the alternating sum of entries of a row of Pascal's triangle is 0.

The fact that the degree of the map is 0 means that the fold count is an interesting quantity. We have an equal number of black and white triangles and so the fold count cannot be too small.

The second result concerns the asymptotics of the fold count (and of another quantity) for the continued fraction colorings. Let  $\{a_n/b_n\} \in (0, 1)$  be a sequence of rationals. Let

$$\mathcal{T}_n = \mathcal{T}(a_n + b_n\alpha), \quad \mathcal{C}_n = \mathcal{C}(a_n + b_n\alpha).$$

Let  $f_n$  denote the fold count of  $\mathcal{C}_n$  and let  $F_n$  denote the number of faces in  $\mathcal{T}_n$ . Let  $R_n$  denote the radius of the largest monochrome disk contained in  $\mathcal{C}_n$ . When  $R_n$  is large, it means that  $\mathcal{C}_n$  contains large totally solid chunks.

**Theorem 1.2** *The following is true about the continued fraction colorings.*

1. *If  $\{a_n/b_n\}$  converges to an irrational limit then  $\lim_{n \rightarrow \infty} f_n/F_n = 0$ .*
2. *If  $\{a_n/b_n\}$  converges to an irrational limit then  $\lim_{n \rightarrow \infty} R_n = \infty$ .*
3. *If  $\{a_n/b_n\}$  is the sequence of continued fraction approximants of a quadratic irrational, then  $\sup\{f_n^2/F_n\} < \infty$ .*

Statement 3 of Theorem 1.2 motivates the following definition.

**Definition:** Given a coloring  $\mathcal{C}$  we define

$$\eta(\mathcal{C}) = \frac{f^2}{F}, \tag{2}$$

where  $f$  is the fold count for  $\mathcal{C}$  and  $F$  is the number of triangles in the triangulation which  $\mathcal{C}$  colors. We call  $\eta(\mathcal{C})$  the *Eisenstein Isoperimetric Ratio* of  $\mathcal{C}$ .

It follows from Theorem 1.1 and the isoperimetric inequality (which for polygons having edges in the 1-skeleton of  $\mathcal{T}$  is stronger by a factor of  $\pi/3$  than the usual isoperimetric inequality) that the continued fraction colorings all have Eisenstein isoperimetric ratio at least 3. More generally, this would hold for any coloring which defines a degree 0 map. The hundreds of random examples I have computed all have this property. This leads to the following conjecture.

**Conjecture 1.3 (Zero Degree)** *Let  $\mathcal{Z}$  be any triangulation of the sphere having degree sequence  $6, \dots, 6, 2, 2, 2$ . Any good coloring of  $\mathcal{Z}$  has the same total number of black and white triangles. Equivalently, any simplicial map from  $\mathcal{Z}$  to the tetrahedron has degree 0.*

The Zero Degree Conjecture makes some intuitive geometric sense. When realized in space, the triangulation  $\mathcal{Z}$  is just the surface of a doubled equilateral triangle – a domain with zero volume. In contrast the tetrahedron bounds a region of positive volume. The simplicial maps don't seem to know anything about these volumes, but maybe they do.

It would follow from the Zero Degree Conjecture and the isoperimetric inequality that any good coloring of a  $6, \dots, 6, 2, 2, 2$  triangulation has Eisenstein isoperimetric ratio at least 3. So, at least conjecturally, some of the continued fraction colorings have the smallest fold counts in a rough sense.

Let me sharpen these statements. Say that *Fibonacci Eisenstein integer* is one where  $a, b$  are consecutive Fibonacci numbers and  $a/b > 1/2$ . Let  $\phi = (1 + \sqrt{5})/2$  be the golden ratio. In §3.3 we will show that

$$\lim_{n \rightarrow \infty} \eta(\mathcal{C}(\beta_n)) = \phi^6 \quad (3)$$

when  $\beta_n$  is the sequence of Fibonacci Eisenstein integers.

Amongst the continued fraction colorings, the Fibonacci examples seem to minimize the Eisenstein Isoperimetric Ratio. Given primitive Eisenstein integers

$$\beta = a + b\alpha, \quad \beta' = a' + b'\alpha,$$

we write  $\beta \preceq \beta'$  if  $b \leq b'$ .

**Conjecture 1.4 (Fibonacci Extremality)**

$$\eta(\mathcal{C}(\beta)) < \eta(\mathcal{C}(\beta')) \quad (4)$$

whenever  $\beta \preceq \beta'$  and  $\beta$  is a Fibonacci Eisenstein integer and  $\beta' \neq \beta$ .

I checked Equation 4 when  $\beta$  is any of the first 10 examples and  $|\beta'| < 500$ . I think that this is very strong evidence. The proof of Equation 4 in general should be purely a matter of number theory. I haven't yet looked for a proof.

Based on the extremal nature of  $\mathcal{C}(2 + 3\alpha)$ , here is a strengthening of Conjecture 1.4.

**Conjecture 1.5 (Fibonacci Isoperimetric Inequality)** *Suppose that  $\beta$  is a Fibonacci Eisenstein integer  $\beta \preceq \beta'$ . Let  $\mathcal{C} = \mathcal{C}(\beta)$ . Let  $\mathcal{C}'$  be an arbitrary good coloring of  $\mathcal{T}(\beta')$ . Then  $\eta(\mathcal{C}) < \eta(\mathcal{C}')$ , with equality if and only if  $\beta' = \beta$  and  $\mathcal{C}'$  is equivalent to  $\mathcal{C}$  up to symmetry and color-reversing.*

This conjecture would combine with Equation 4 to prove the following general conjecture.

**Conjecture 1.6 (Asymptotic Isoperimetric Inequality)** *Suppose that  $\{\mathcal{G}_n\}$  is any infinite sequence of distinct colorings of sphere triangulations with degree sequence  $6, \dots, 6, 2, 2, 2$ . Then  $\liminf_{n \rightarrow \infty} \eta(\mathcal{G}_n) \geq \phi^6$ .*

Equation 3 says that this conjectured isoperimetric inequality is sharp.

## 1.4 Organization

In §2, after a discussion of the slow Gauss map and its connection to continued fractions, I will launch into the construction of the  $\mathcal{C}(\cdot)$  family. The building blocks are what I call *capped flowers*, and these in turn are made in layers from cyclically arranged patterns of trapezoids which I call *trapezoid necklaces*. (Look again at Figure 1.) I will explain how the set of trapezoid necklaces is naturally the vertex set of the infinite rooted binary tree (modified to have an extra vertex at the bottom). Taking a path in this tree defines the capped flower. In §3 I will prove Theorems 1.1 and 1.2 and establish Equation 3.

## 1.5 Acknowledgements

I'd like to thank Ethan Bove, Peter Doyle, Jeremy Kahn, Rick Kenyon, Curtis McMullen, and Peter Smillie for various conversations (sometimes going back some years) on topics related to the material here.



## 2 The Main Construction

### 2.1 The Slow Gauss Map

Let  $\mathcal{S}$  denote the set of rational numbers in the interval  $(0, 1]$ . The *slow Gauss map* is the following map from  $\mathcal{S} - \{1\}$  into  $\mathcal{S}$ :

$$\gamma\left(\frac{a}{a+b}\right) = \gamma\left(\frac{b}{a+b}\right) = \frac{a}{b}. \quad (5)$$

The number  $1/2$  is the only element that  $\gamma$  maps to  $1 = 1/1$ . Otherwise each number has 2 pre-images. Given the map  $\gamma$ , we can think of  $\mathcal{S}$  as the infinite rooted binary tree (modified to have an extra bottom vertex). We make this tree by joining each member of  $\mathcal{S} - \{1\}$  to its image under  $\gamma$ . Figure 2 shows the beginning of this tree.

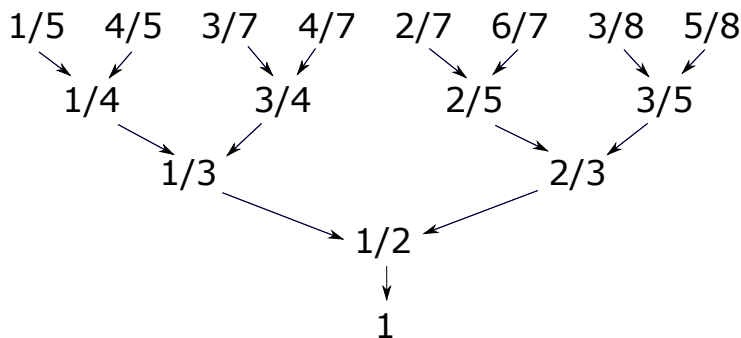


**Figure 2:** The beginning of the tree of rationals.

We work entirely with the slow Gauss map, but we explain how this map is connected to continued fractions. The traditional Gauss map is defined to be

$$\gamma^*(p/q) = (q/p) - \text{floor}(q/p). \quad (6)$$

For each  $p/q$  there is some *comparison exponent*  $k$  such that

$$\gamma^*(p/q) = \gamma^k(p/q).$$

In other words, the (suitably) iterated slow Gauss map has the same action as the traditional Gauss map; it just works more slowly. The continued fraction expansion of  $p/q$  is derived from recording the sequence of comparison exponents we see as we iteratively apply  $\gamma$  and  $\gamma^*$  to  $p/q$ . I will discuss this again more geometrically at the end of §2.3.

## 2.2 Trapezoid Necklaces

An *isosceles trapezoid* is a quadrilateral with two parallel sides such that the other two sides are non-parallel but have the same length. We call the longer parallel side the *top*, the shorter parallel side the *bottom*, and the other two sides the *diagonal sides*. We allow the degenerate case of an isosceles triangle. In this case the bottom has length 0. An *Eisenstein trapezoid* is an isosceles trapezoid whose edges lie in the 1-skeleton of  $\mathcal{T}$ , the planar equilateral triangulation whose vertices are the Eisenstein integers. Figure 1 above and Figure 3 below feature some Eisenstein trapezoids.

Up to symmetries of  $\mathcal{T}$ , an Eisenstein trapezoid  $X$  is characterized by the pair  $(a, b)$  where  $a$  is the length of a diagonal side of  $X$  and  $b$  is the length of the top. We call  $X$  *primitive* if  $a, b$  are relatively prime. When  $X$  is primitive, we define the *aspect ratio* to be  $a/b$ . The aspect ratio determines the primitive Eisenstein trapezoid up to symmetries of  $\mathcal{T}$ . Thus, modulo symmetry the primitive Eisenstein trapezoids are naturally in bijection with the set  $\mathcal{S}$  of rationals considered above. The Eisenstein trapezoids in Figure 1 are all primitive, and their aspect ratios are variously  $1/1$  and  $1/2$  and  $2/3$ . The Eisenstein trapezoids in Figure 3 have aspect ratio  $3/5$ .

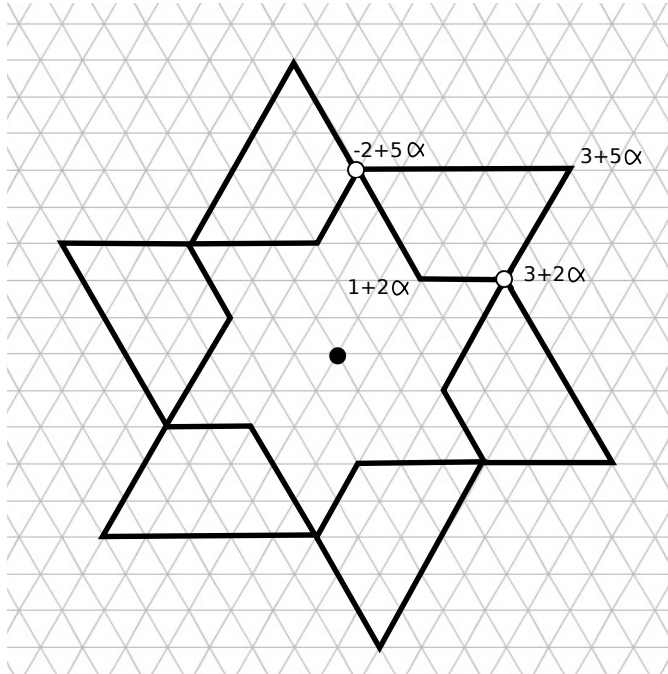


**Figure 3:** A trapezoid necklace of aspect ratio  $3/5$ .

Figure 3 illustrates what we mean by a *trapezoid necklace*. This is a union of 6 primitive Eisenstein trapezoids  $X_1, \dots, X_6$  which has the following properties:

- The trapezoids have pairwise disjoint interiors.
- $X_i \cap X_{i+1}$  is a single point, a common vertex, for all  $i$ .
- An order 6 rotation  $\rho$  of  $\mathcal{T}$  has the action  $\rho(X_i) = X_{i+1}$  for all  $i$ .

In this description the indices are taken mod 6. We define the *center* of the necklace to be the fixed point of  $\rho$ . When the center is 0, the map  $\rho$  (or perhaps its inverse) is multiplication by  $\alpha$ . We define the aspect ratio of the necklace to be the common aspect ratio of the 6 individual trapezoids.

Up to symmetry of  $\mathcal{T}$ , there exists a unique Eisenstein necklace of aspect ratio  $a/b \in \mathcal{S}$ . If we normalize the picture so that 0 is the center, then one of the trapezoids  $X_1$  has vertices

$$a + b\alpha, \quad (a - b) + b\alpha, \quad (2a - b) + (b - a)\alpha, \quad a + (b - a)\alpha.$$

The intersection of  $X_1$  and  $X_2 = \rho(X_1)$  is the point  $(a - b) + b\alpha$  because

$$\alpha \times (a + (a - b)\alpha) = (a - b) + b\alpha.$$

This little calculation uses the fact that  $\alpha^2 = \alpha - 1$ .

### 2.3 Empty Trapezoid Flowers

Each trapezoid necklace  $X$  defines a smaller trapezoid necklace  $Y = \gamma(X)$  having the same center. The defining property is that the top side of each trapezoid  $Y_i$  in  $Y$  is a side of a trapezoid  $X_j$  of  $X$ , and one of the diagonal sides of  $Y_i$  is a side of one of the trapezoids of  $X$  adjacent to  $X_j$ . This awkward definition is very much like a written description of how to drink a glass of water. A demonstration says a thousand words. Figure 4 shows the trapezoid necklaces

$$X \rightarrow \gamma(X) \rightarrow \gamma^2(X) \rightarrow \gamma^3(X)$$

alternately colored black and white. Here  $X$  is as in Figure 3. The respective aspect ratios are given by  $3/5 \rightarrow 2/3 \rightarrow 1/2 \rightarrow 1/1$ . We call the union of these necklaces the *empty 3/5-flower*.

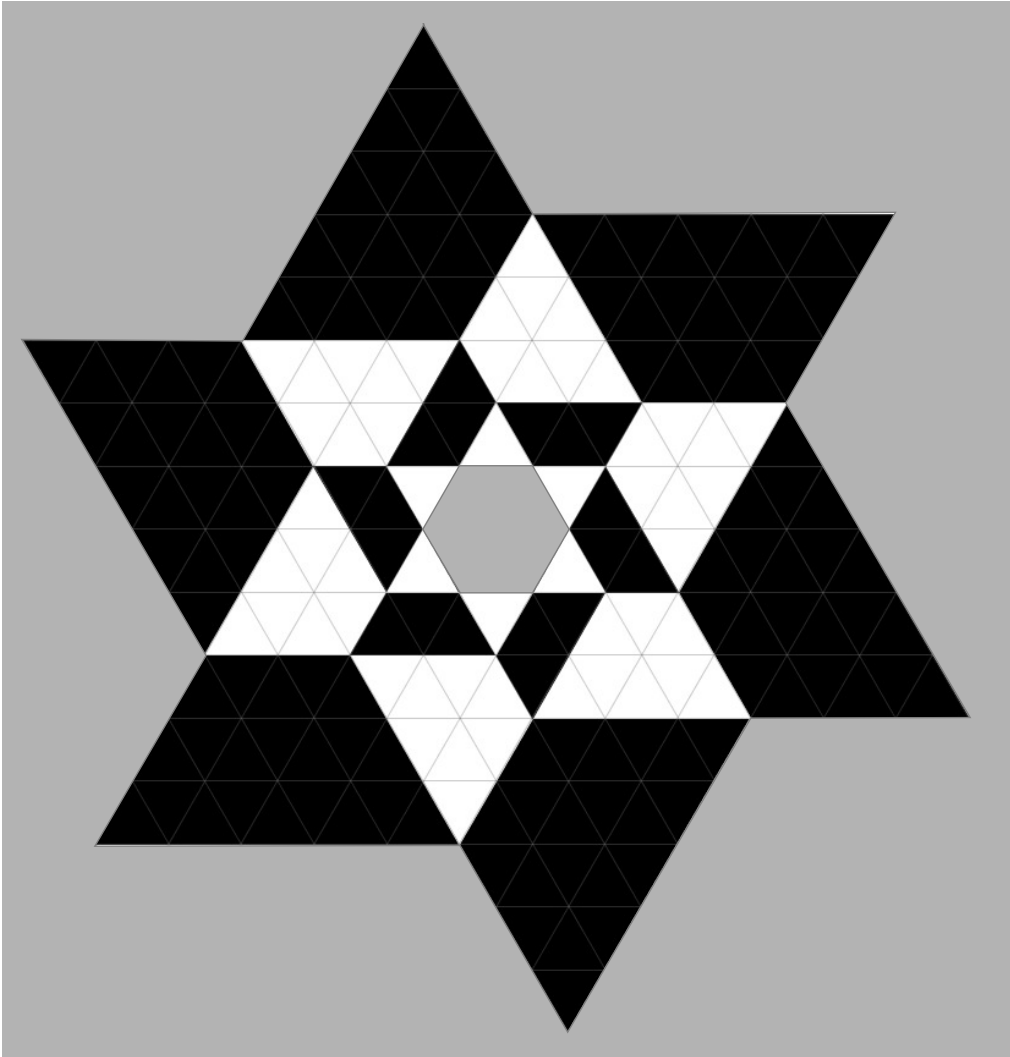


**Figure 4:** The empty 3/5-flower.

As is suggested by our notation, the action of  $\gamma$  here mirrors the action of the slow Gauss map  $\gamma$  from the previous section. That is, if  $r$  is the aspect ratio of  $X$  then  $\gamma(r)$  is the aspect ratio of  $\gamma(X)$ . Our construction mirrors the action of the slow Gauss map.

We discussed above how the slow Gauss map is related to continued fractions. Here we continue the discussion. As we now illustrate, our construction also precisely implements the continued fraction expansion.

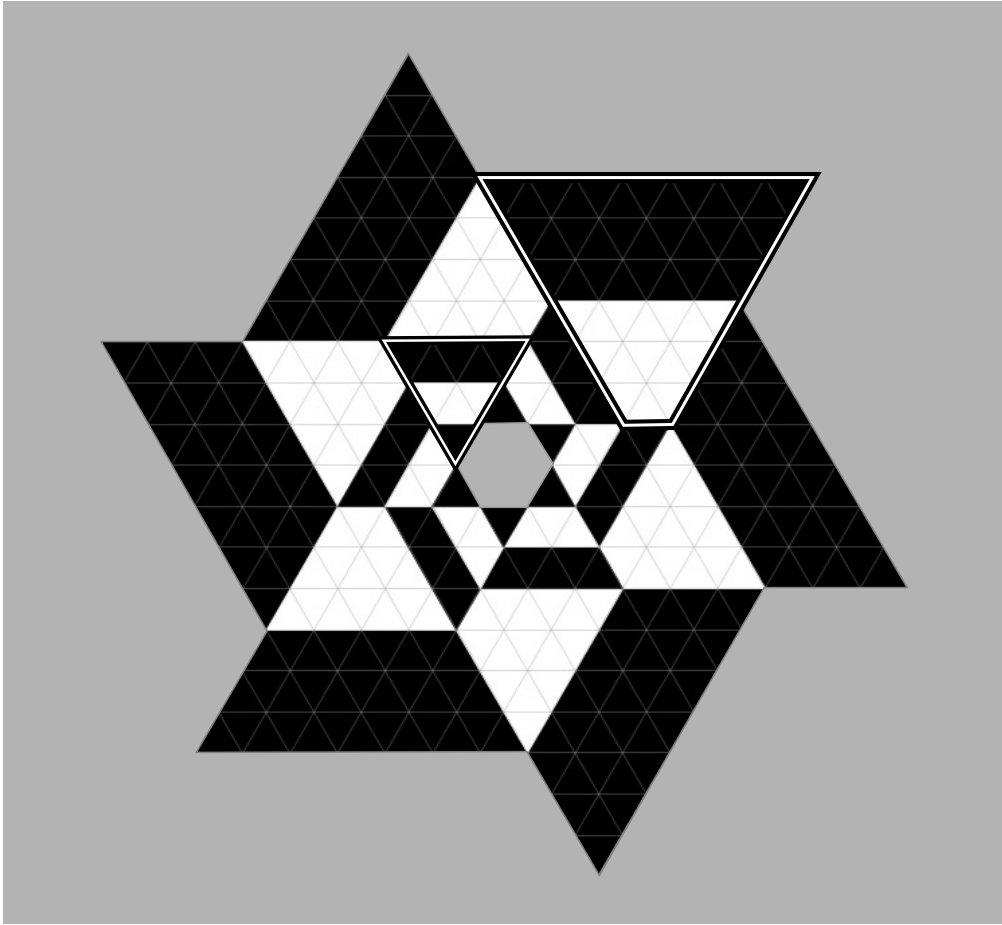


**Figure 5:** The empty  $3/7$ -flower.

Figure 5 shows the empty  $3/7$ -flower, corresponding to the tree path  $3/7 \rightarrow 3/4 \rightarrow 1/3 \rightarrow 1/2 \rightarrow 1/1$ . The specially-outlined trapezoids (and their rotated images) are the maximal trapezoids in the flower. They have respectively 2 and 3 “stripes”. For comparison,  $3/7$  has continued fraction  $0 : 2 : 3$ . That is

$$\frac{3}{7} = 0 + \frac{1}{2 + \frac{1}{3}}.$$

In general, the empty  $p/q$ -flower starts with a  $p/q$ -necklace and then fills in the full  $\gamma$  orbit, alternately coloring the necklaces black and white. The innermost necklace always has aspect ratio  $1/1$ . Up to symmetries of  $\mathcal{T}$ , the empty  $p/q$ -flower is unique. One can read off the continued fraction expansion of  $p/q$  by counting the stripes of the maximal trapezoids.

## 2.4 Filling and Capping the Flowers

We fill an empty flower by coloring the remaining 6 triangles black and white in an alternating pattern. Figure 6 shows this for the  $3/5$ -flower. Up to symmetries of  $\mathcal{T}$  (and swapping the colors) there is a unique  $p/q$ -flower. The empty flowers have 6-fold rotational symmetry but the (filled) flowers have 3-fold rotational symmetry. We break a symmetry to define the filling.

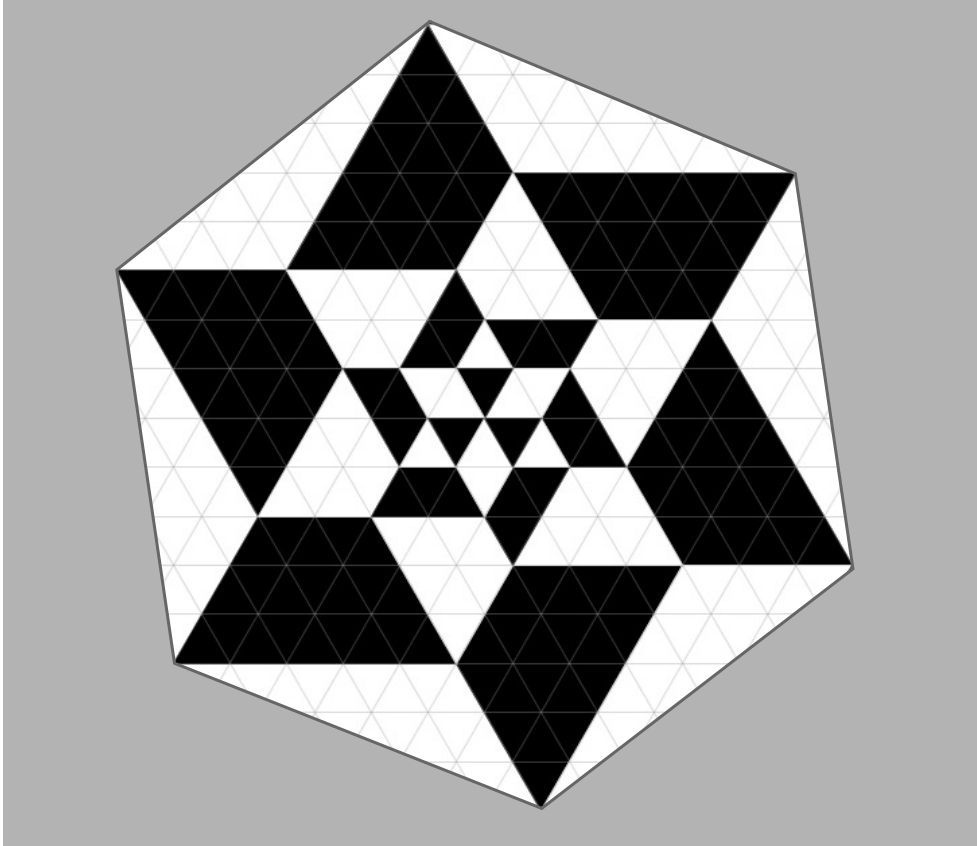


**Figure 6:** The filled and capped  $3/5$ -flower

Figure 6 also shows what we mean by *capping* a flower. We take the convex hull of the flower and color the complementary triangles the color opposite the color of the outer necklace. The capped flowers, which are regular hexagons with Eisenstein integer vertices, are the building blocks of our colorings. When two translation-equivalent capped flowers meet along a common boundary edge, the triangular regions merge to become an *Eisenstein parallelogram* – i.e., one whose boundary lies in the 1-skeleton of  $\mathcal{T}$ .

## 2.5 Defining the Colorings

Consider the hexagonal tiling of the plane by translates of the capped  $a/b$ -flower. Because the capped flowers have 3-fold rotational symmetry, the resulting planar coloring is invariant under the group  $G_\beta$  generated by order 3 reflections in the vertices and centers of the hexagons. The quotient of this planar coloring by  $G_\beta$  is  $\mathcal{C}(\beta)$ . By construction,  $\mathcal{C}(\beta)$  is good.

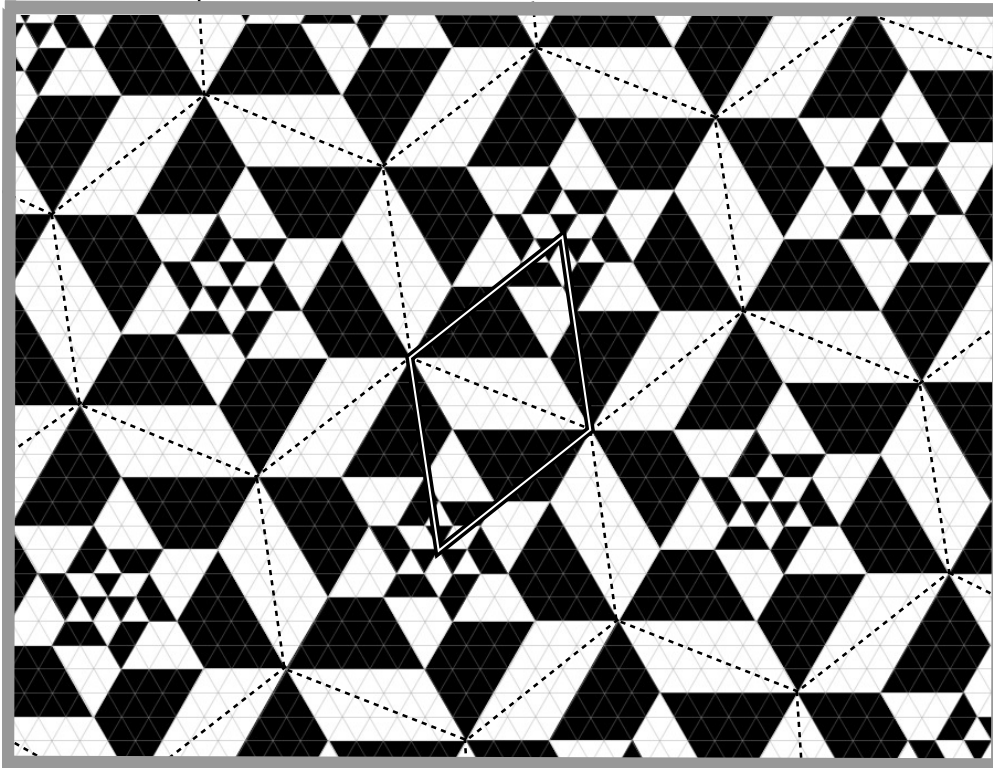


**Figure 7:** The universal cover of  $\mathcal{C}(3 + 5\alpha)$ .

Figure 7 shows the construction for  $\beta = 3 + 5\alpha$ . The region bounded by the big central rhombus is a fundamental domain for the action of  $G_\beta$ . The colorings exhibit a lot of variety. Figure 8 below shows  $\mathcal{C}(a + 13b)$  for  $a = 1, 3, 5, 7, 9, 11$ . It is worth noting that for parameters like  $1/13$  the fold count is linear in the number of triangles.

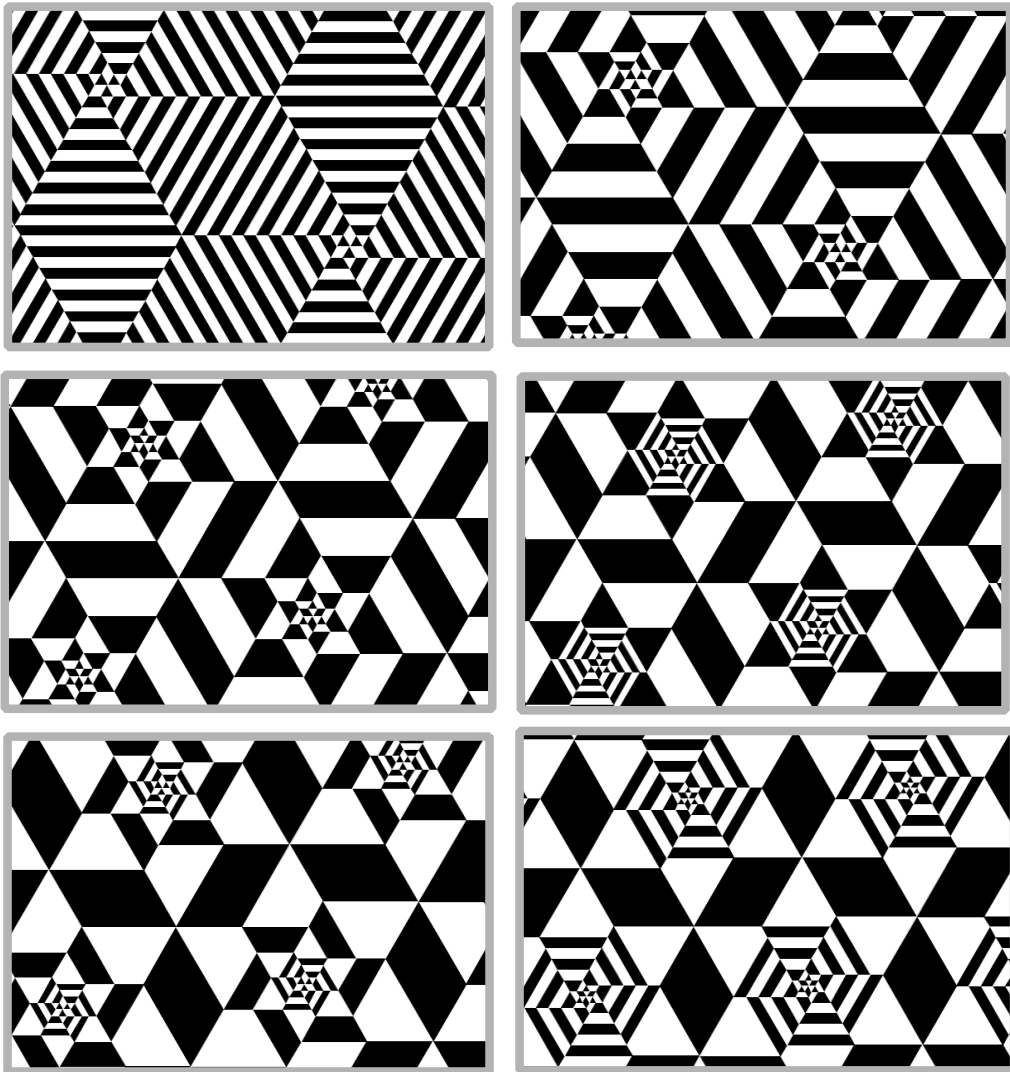


**Figure 8:** The covers of  $\mathcal{C}(a + 13\alpha)$  for  $a = 1, 3, 5, 7, 9, 11..$



### 3 Properties of the Colorings

#### 3.1 The Zero Degree Property

In this section we prove Theorem 1.1.

Let  $A(a/b)$  denote the number of equilateral triangles in the trapezoid of aspect ratio  $a/b$ . An easy calculation shows that

$$A(a/b) = 2ab - a^2. \tag{7}$$

Let

$$\frac{a}{b} = \frac{a_n}{b_n} \rightarrow \dots \rightarrow \frac{a_0}{b_0} = \frac{1}{1}$$

be some branch of the rational binary tree. After we have suitably permuted the colors, the number of black and white triangles in  $\mathcal{C}(a + b\alpha)$  respectively are

$$N_1(a/b) = 1 + 2A(a_n/b_n) + 2A(a_{n-2}/b_{n-2}) + 2A(a_{n-4}/b_{n-4}) + \dots$$

and

$$N_2(a/b) = 1 + 2a_nb_n + 2A(a_{n-1}/b_{n-1}) + 2A(a_{n-3}/b_{n-3}) + \dots$$

We want to see that  $N_1(a/b) = N_2(a/b)$ .

Before we give the general argument, let us work out the example from Figure 1, namely

$$\frac{2}{3} \rightarrow \frac{1}{2} \rightarrow \frac{1}{1}.$$

The two sums above are

$$N_1(2/3) = 1 + 16 + 2 = 19, \quad N_2(2/3) = 1 + 12 + 6 = 19.$$

So in this example the two sums are equal.

In general the proof goes by induction. We want to see that

$$N(a/b) = N_2(a/b) - N_1(a/b) = 0.$$

Suppose we augment our path of rationals as follows:

$$\frac{a}{a+b} = \frac{a_n}{a_n+b_n} \rightarrow \frac{a_n}{b_n} \rightarrow \dots \rightarrow \frac{1}{1},$$

Suppose also that we keep the inner necklaces the same color so that the roles of  $N_1$  and  $N_2$  switch when we are comparing the two cases. Only the outermost layers change, so to speak, and we compute

$$\begin{aligned} N\left(\frac{a}{a+b}\right) - N\left(\frac{a}{b}\right) &= 2ab + 2a(a+b) - 2A\left(\frac{a}{a+b}\right) = \\ &= 2ab + 2a^2 + 2ab - 4a(a+b) + 2a^2 = 0. \end{aligned}$$

If we instead augment our path by  $b/(a+b)$  then

$$\begin{aligned} N\left(\frac{a}{a+b}\right) - N\left(\frac{a}{b}\right) &= 2ab + 2b(a+b) - 2A\left(\frac{b}{a+b}\right) = \\ &= 2ab + 2ab + 2b^2 - 4b(a+b) + 2b^2 = 0. \end{aligned}$$

This completes the induction proof.

## 3.2 Asymptotic Properties

In this section we prove Theorem 1.2.

Now suppose that  $\{p_n/q_n\}$  is an infinite sequence of elements of  $\mathcal{S}$  having an irrational limit  $\psi$ . The continued fraction expansions of these numbers converge to the continued fraction expansion of  $\psi$ . This means that for any  $D$  there are constants  $M, N$  such that if  $n > N$  then all but the first  $M$  terms of  $p_n/q_n$  have  $p_n > D$ . In terms of the flowers, all but the first  $M$  inner trapezoid necklaces  $Q$  have the property that

$$\frac{p(Q)}{A(Q)} < \frac{100}{D}.$$

Here  $p(Q)$  denotes the perimeter of  $Q$  and, as above,  $A(Q)$  denotes the number of equilateral triangles comprising  $Q$ . We picked an unrealistically large constant of 100 here to avoid having to think about the fine points of trapezoids.

Our analysis shows that, within the  $n$ th flower, the average ratio of the perimeter of a trapezoid to the area of the trapezoid tends to 0 as  $n \rightarrow \infty$ . This immediately implies that the ratio  $f_n/F_n$  converges to 0. This is the first property.

The second property is immediate. The big and fat trapezoids in our flowers will contain big monochrome disks.

For the third property, we observe that a quadratic irrational has a periodic continued fraction approximation. The fact that the continued fraction expansion is periodic translates into the fact that our flowers are asymptotically self-similar. There is an asymptotic scaling factor  $\lambda > 1$  such that multiplication by  $\lambda^{-1}$  preserves the flower up to a uniformly bounded discrepancy.

Hence, up to a bounded error, the sequence of perimeters of the successive necklaces looks like

$$c_1, \dots, c_k, \lambda c_1, \dots, \lambda c_k, \lambda^2 c_1, \dots, \lambda^2 c_k, \dots$$

for some constants  $c_1, \dots, c_k$ , up to a uniformly bounded error in each term. Hence  $f_n = C_n \lambda^{n'}$  for some sequence  $\{C_n\}$  that is bounded away from both 0 and  $\infty$ . Here  $n'$  is the length of the  $\gamma$ -orbit of  $p_n/q_n$ , divided by  $k$ . At the same time, the corresponding sequence of areas looks like

$$a_1, \dots, a_k, \lambda^2 a_1, \dots, \lambda^2 a_k, \lambda^4 a_1, \dots, \lambda^4 a_k, \dots$$

up to a uniformly bounded error in each term. This means that  $F_n = C'_n \lambda^{2n'}$  for some other sequence  $\{C'_n\}$  that is also bounded away from 0 and  $\infty$ . Putting these two estimates together, we see that  $f_n^2/F_n = C_n^2/C'_n$  is uniformly bounded.

### 3.3 The Fibonacci Case

In this section we establish Equation 3.

Recall that  $\eta = f^2/F$  is the Eisenstein isoperimetric ratio. Let

$$(a_1, a_2, a_3, a_4, a_5, \dots) = (1, 1, 2, 3, 5, \dots)$$

be the sequence of Fibonacci numbers. Let  $\phi = (1 + \sqrt{5})/2$  be the golden mean. We first note the well-known asymptotic

$$a_n \sim \frac{\phi^n}{\sqrt{5}}. \tag{8}$$

The difference tends to 0 exponentially fast in  $n$ .

Let  $f_n$  be the fold count for  $\mathcal{C}(a_n + a_{n+1}\alpha)$  and let  $F_n$  be the number of faces. Let  $\eta_n$  be the Eisenstein Isoperimetric Ratio of  $\mathcal{C}(a_n + a_{n+1}\alpha)$ . Just as a check for our general formula, we first record some special cases.

$$(f_1, f_2, f_3, f_4, f_5) = (7, 13, 23, 39, 65),$$

$$(F_1, F_2, F_3, F_4, F_5) = (6, 14, 38, 98, 258).$$

These values yield

$$(\eta_1, \eta_2, \eta_3, \eta_4, \eta_5) = (8.16\dots, 12.07\dots, 13.92\dots, 15.52, \dots, 16.38\dots).$$

In general, we have

$$f_n = -1 + 2 \sum_{k=1}^{n+2} a_k, \quad F_n = 2 + 4 \sum_{k=1}^n a_k a_{k+1}. \quad (9)$$

These formulas give the same answers as the lists above for  $n = 1, 2, 3, 4, 5$ , and the same kind of inductive proof as the one given in §3.1 establishes them.

Using the approximation in Equation 8, and the familiar formula for the partial sums of a geometric series, and the fact that  $1 + \phi = \phi^2$ , we find that

$$f_n^2 \approx \frac{4}{5} \times \phi^{2n+8}, \quad F_n \approx \frac{4}{5} \times \phi^{2n+2}.$$

Here  $\approx$  means equal up to a uniformly bounded error. Dividing the one equation by the other gives Equation 3.

## 4 References

[**T**], W. P. Thurston, *Shapes of Polyhedra*, arXiv:math/9801088 (1998)

[**W**], D. B. West, *Introduction to Graph Theory, 2nd Ed.*, Prentice-Hall (2000)